

THE PENNSYLVANIA STATE UNIVERSITY  
SCHREYER HONORS COLLEGE

DEPARTMENT OF BIOCHEMISTRY AND MOLECULAR BIOLOGY

Characterizing rescue of an Alzheimer's disease model in *Drosophila* by downregulation of  
heparan sulfate biosynthetic enzymes and treatment by bosutinib

LINDSEY SWANSON  
SPRING 2024

A thesis  
submitted in partial fulfillment  
of the requirements  
for a baccalaureate degree  
in Biology  
with honors in Biochemistry and Molecular Biology

Reviewed and approved\* by the following:

Scott Selleck  
Professor of Biochemistry and Molecular Biology  
Thesis Supervisor

Sarah Assmann  
Waller Professor of Biology  
Honors Adviser

\* Electronic approvals are on file.

## ABSTRACT

Alzheimer's disease (AD) is a neurodegenerative disorder characterized by memory loss, cognitive decline, and behavioral changes. The most common causes of familial, early-onset AD are related to mutations in *presenilin-1* (*PSEN1*). The *PSEN1* gene encodes for presenilin-1 protein, which is a major component of the  $\gamma$ -secretase complex. This is a protease complex involved in the cleavage of transmembrane proteins. About 90% of these *PSEN1* mutations are reduction or loss-of-function, and they lead to detrimental changes within cells including decreased autophagy, mitochondrial dysfunction, and abnormal lipid accumulation. Previous studies have analyzed the function of heparan sulfate-modified proteoglycans (HSPGs) in cellular pathways and their effect on AD pathology. HSPGs are found at the cell surface and in the extracellular matrix and play a critical role in growth factor action. The gene *NDST1* affects the sulfation level of HS, and it has been shown that downregulating *NDST1* decreases the sulfation of HS and counteracts the negative autophagic, mitochondrial, and lipid effects induced by *PSEN1* downregulation. Additionally, bosutinib, an FDA-approved drug for chronic myelogenous leukemia, has also been shown to have counteractive effects similar to *NDST1* but through a tyrosine kinase inhibiting pathway. The purpose of these experiments was to study the relationship between presenilin and sulfation levels as well as between presenilin and bosutinib in a *Drosophila* model and attempt to rescue the diseased state in these animals. This was done by knocking down *Psn*, a homolog of *PSEN1*, and *sulfateless* (*sfl*), a homolog of *NDST1*. Knocking down *Psn* led to abnormalities in mitochondria and liposome morphology. Both methods of attempted rescue- introducing a simultaneous knockdown of *sfl* and treating diseased flies with bosutinib- suppressed these effects to different degrees.

## TABLE OF CONTENTS

LIST OF FIGURES .....	iii
ACKNOWLEDGEMENTS .....	iv
Chapter 1 Introduction .....	1
Autophagy .....	1
Mutations in presenilin .....	3
Heparan sulfate-modified proteoglycans .....	5
Screening for bosutinib as a treatment .....	7
<i>UAS-Gal4</i> System .....	8
Chapter 2 Materials and methods .....	10
Experimental design .....	10
<i>Drosophila</i> husbandry .....	12
Preparation of bosutinib in food .....	13
MitoTracker™ Red staining of fat bodies .....	14
LipidTox™ Red staining of fat bodies .....	14
Confocal microscopy .....	15
Statistical analysis .....	15
Chapter 3 Results .....	17
<i>Sft</i> <sup>03844</sup> knockdown rescues <i>Psn3</i> <sup>RNAi</sup> -mediated abnormalities in mitochondria .....	17
Treatment with bosutinib rescues <i>Psn3</i> <sup>RNAi</sup> -mediated abnormalities in mitochondria ....	20
<i>Sft</i> <sup>RNAi</sup> impacts <i>Psn3</i> <sup>RNAi</sup> -mediated alterations in liposome morphology .....	23
Treatment with bosutinib impacts <i>Psn3</i> <sup>RNAi</sup> -mediated alterations in liposome morphology	25
Chapter 4 Discussion .....	27
Dysfunction of mitochondria and lipid metabolism are implicated in AD .....	27
Decreasing heparan sulfate improves AD pathology .....	28
Bosutinib as a potential treatment of AD .....	30
Limitations .....	31
Future directions .....	32
Chapter 5 Conclusion .....	35
BIBLIOGRAPHY .....	36

## LIST OF FIGURES

Figure 1. Steps of Macroautophagy .....	2
Figure 2. Heparan sulfate-modified proteoglycan structure .....	5
Figure 3. Relationship between UAS-Gal4 and RNAi .....	9
Figure 4. <i>Psn3<sup>RNAi</sup></i> and <i>sfl<sup>03844</sup></i> downregulation alter mitochondrial number and morphology in fat body cells and double knockdown suppresses <i>Psn3<sup>RNAi</sup></i> -induced changes .....	18
Figure 5. Line graph of MitoTracker™ Red intensity distribution in <i>Drosophila</i> fat body cells with knockdown of <i>sfl<sup>03844</sup></i> , <i>Psn3<sup>RNAi</sup></i> , or <i>Psn3<sup>RNAi</sup>;sfl<sup>03844</sup></i> .....	19
Figure 6. <i>Psn3<sup>RNAi</sup></i> alters mitochondrial number and morphology in fat body cells and treatment with bosutinib suppresses <i>Psn3<sup>RNAi</sup></i> -induced changes.....	21
Figure 7. Line graph of MitoTracker™ Red intensity distribution in <i>Drosophila</i> fat body cells treated with bosutinib .....	22
Figure 8. <i>Sfl<sup>RNAi</sup></i> partially reverts <i>Psn3<sup>RNAi</sup></i> -mediated changes in liposome morphology .....	24
Figure 9. Treatment with bosutinib partially reverts <i>Psn3<sup>RNAi</sup></i> -mediated changes in liposome morphology .....	26

## ACKNOWLEDGEMENTS

I would first like to thank my principal investigator Dr. Scott Selleck for giving me the opportunity to work in his lab and contribute to his research in Alzheimer's disease as well as for being my thesis supervisor. This past year has been an invaluable experience that has immensely improved my skills in conducting research, thinking critically, and growing as a biologist.

Secondly, I would like to thank Nicholas Schultheis, the graduate student in the Selleck Lab, for teaching me everything I know about *Drosophila* husbandry, dissection, and imaging. Despite being busy with his own studies, he has always gone out of his way to give me biochemistry lessons, teach me procedures, or just be someone to lean on. He has made the lab a welcoming environment and a place that I look forward to going to everyday, and this thesis would not have been possible without his continuous support and encouragement.

I would also like to thank the rest of the members of the Selleck Lab- Alyssa Connell, Sophia DeGuara, Grace O'Sullivan, Jolyn Toyomura, and Uzair Alam- for always making lab the best part of my day. They are incredible scientists and some of my best friends.

Lastly, I would like to thank my parents, Traci and Craig Swanson, as well as the rest of my family and friends for their endless support throughout my education and life in general. I would not be where I am today without them, and I will always be grateful for the wonderful support system that I have.

## **Chapter 1**

### **Introduction**

Alzheimer's disease (AD) is the most common type of dementia, affecting about 6 million people in the United States. Discovered by Dr. Alois Alzheimer in 1906, AD is associated with behavioral symptoms including memory loss, cognitive decline, language difficulty, and unpredictable behavior. It is also characterized by pathological manifestations such as the accumulation of amyloid plaque and tangled neurofibrillary bundles known as tau tangles in the brain, as well as a loss of neuronal connections.<sup>1</sup> Historically, attempts at treating AD have mainly involved targeting these amyloid plaques, but little to modest progress has been made with that approach. The Selleck Lab is interested in other cellular deficits that appear to be earlier and possibly more direct causes of AD deficits. Some of these include reduced autophagy, damaged mitochondria, and lipid accumulation, and attempts at rescuing this disease in the Selleck Lab have been focused on these other cellular mechanisms.

### **Autophagy**

One of the main targets that the Selleck Lab has identified in improving AD outcomes has been the regulation of autophagy. Autophagy is the body's self-degrading process in which unnecessary or damaged components of a cell, such as proteins, mitochondria (through mitophagy), and lipids (through lipophagy), are degraded by lysosomes to recycle cell building blocks and produce healthier cellular structures. Macroautophagy is the type of autophagy that is

of concern when it comes to AD since a decreased rate of macroautophagy is observed in the disease's pathology. In this process, an isolation membrane called a phagophore forms, which then elongates and closes to form a vacuole around whatever must be degraded, creating an autophagosome. The autophagosome then transports that material to a lysosome, and the autophagosome and lysosome fuse to form an autophagolysosome. From there, the contents within the fused membrane are lysed or broken down.<sup>2</sup> Pictured below is a visual of the basic steps of macroautophagy.

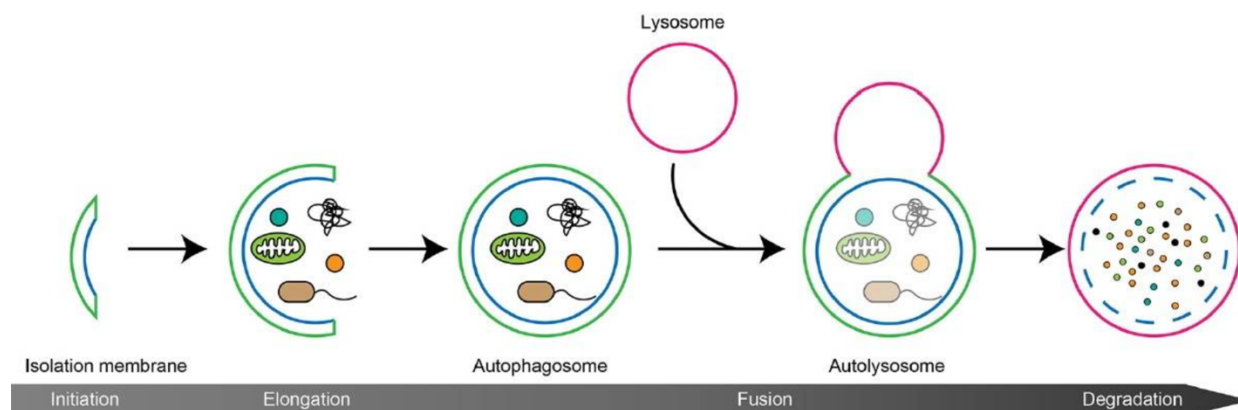


**Figure 1. Steps of Macroautophagy**

This figure depicts the basic steps of macroautophagy: initiation, elongation, fusion, and degradation. An isolation membrane forms and elongates around the contents to be degraded, creating an autophagosome. After fusing with a lysosome, an autolysosome/autophagolysosome is formed. Finally, the contents are lysed or degraded. Figure from Nakamura & Yoshimori, 2018.<sup>4</sup>

Autophagy dysfunction is related to the onset and progression of AD because if autophagy is not occurring properly, this can lead to the buildup of damaged mitochondria, lipids, and proteins including  $\beta$ -amyloid and Tau. Mitochondrial function is connected to autophagic processes because damaged mitochondria are removed by autophagy, which prevents

the spread of damaging reactive oxygen species to other organelles. Healthy mitochondria are also necessary for lipid metabolism since they break down fatty acids through  $\beta$ -oxidation and provide the ATP necessary to carry out other catabolic processes within the cell.<sup>3</sup> By inhibiting anabolic pathways that contribute to the buildup of these damaged cellular structures, catabolic processes can be allowed to increase, which can elevate the rate at which these damaged organelles and proteins are broken down. This, therefore, can help combat the issues of lipid accumulation, protein aggregation, and mitochondrial dysfunction that are observed in AD. One of the ways in which anabolism can be inhibited is by lowering the level of sulfation on heparan sulfate, a coreceptor for growth factors and growth factor receptors.

It has previously been shown that in patients with AD, the fusion of autophagosomes with lysosomes is hindered, and a buildup of autophagosomes and autophagic vacuoles, which are intermediates in autophagy, has been observed.<sup>5</sup> This means that autophagy is being initiated, but something involved in autophagolysosome formation is interfering with it being carried out to completion. This is where *PSEN1* dysfunction comes into play. *PSEN1* is one of the main genes that when mutated is associated with AD, but it also plays a large role in autophagy and in this autophagolysosome formation step.

### **Mutations in presenilin**

Familial, early-onset Alzheimer's disease is most commonly associated with mutations in *presenilin-1 (PSEN1)*. *PSEN1* encodes for the protein presenilin-1, which is a major component of the  $\gamma$ -secretase complex. This is a protease complex involved in the cleavage of transmembrane proteins. *PSEN1* mutations are dominantly inherited and typically lead to

cognitive decline starting in the fourth decade of life.<sup>3</sup> About 90% of these *PSENI* mutations are reduction or loss-of-function, which reduces the activity of the  $\gamma$ -secretase complex and suggests that this is related to the onset of AD.<sup>5</sup>

*PSENI* plays a large role in autophagy, which could explain in part why mutations in it are so heavily linked to AD onset. One of its functions is to target the V-ATPase subunit to lysosomes. V-ATPase, or vacuolar ATPase, is an ATP-driven proton pump that functions in pumping protons into the lysosome to make it acidic.<sup>6</sup> Without these acidic conditions, certain proteases cannot become activated to degrade the autophagolysosome contents. Therefore, if *PSENI* undergoes a reduction or loss-of-function mutation, autophagolysosomes cannot be properly formed, lysosomes cannot reach the conditions necessary for autophagy, autophagy decreases, and thus damaged mitochondria, lipids, and proteins accumulate.

Because it is known that loss-of-function mutations in *PSENI* are the main determinant of early-onset AD in humans, we have created a similar model of AD in *Drosophila* by knocking down *Psn*, the homolog of *PSENI*. Our model utilized an RNA interference (RNAi) construct to reduce the function of *Psn*. RNAi is a method of reducing gene expression by transcribing a hairpin loop of mRNA, which is formed from an mRNA strand folding on itself to form base pairs with another section of that strand. This causes the RNA-induced silencing complex to cleave any cellular mRNA that is complementary to one of the strands of the hairpin loop.<sup>7</sup> Therefore, by using a *Psn*<sup>RNAi</sup> model, the mRNA of *Psn* is decreased.

These experiments used the variant *Psn*<sup>3<sup>RNAi</sup>, which is one of the sequences of targets for *Psn* that reduces *Psn* function by roughly 30%. This modest reduction has been shown in our lab to have significant detrimental effects on *Drosophila*, including an increase in number of</sup>

vacuoles in adult brains, negative behavioral changes, smaller and fewer mitochondria, and amorphous liposomes, all phenotypes that are characteristic of AD.<sup>3</sup>

### Heparan sulfate-modified proteoglycans

Heparan sulfate-modified proteoglycans (HSPGs) are found on the cell surface and in the extracellular matrix, and one of their functions is to act as a coreceptor for growth factors and growth factor receptors.<sup>3</sup> Their structure consists of a protein core and one or more covalently linked side chains of heparan sulfate (HS). HS is a linear polysaccharide found in all animal tissues that is composed of the repeating, highly sulfated disaccharide units *N*-acetyl-*D*-glucosamine and *D*-glucuronic acid.<sup>8</sup> Pictured below is a simplified model of a HSPG.

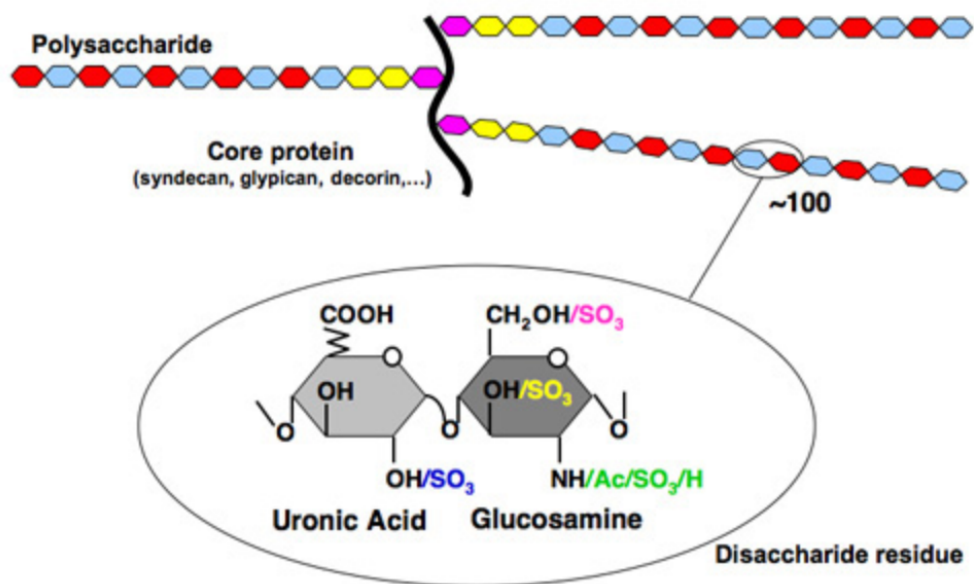


**Figure 2. Heparan sulfate-modified proteoglycan structure**

This is a highly simplified illustration of HSPGs depicting the core protein and disaccharide chain. Figure from Balagurunathan, 2024.<sup>9</sup>

HSPGs regulate signaling events and the activity of protein growth factors, and the level of sulfation on HS impacts the extent to which they do this by impacting properties like binding affinity and selectivity. By decreasing the chain length or sulfation level of HS through the downregulation of HS biosynthetic enzymes, autophagy in muscle and fat body cells of *Drosophila* has been found to be increased<sup>10</sup>, which makes sense because growth factors are being inhibited. Suppressing these anabolic processes promotes catabolic processes and results in a net increase of autophagic flux beyond the level that occurs in healthy, wildtype animals. Coupling this effect with that of *Psn* downregulation, though, could help counteract the accumulation of damaged cellular structures observed in AD and aid in restoring a healthy ratio between anabolism and catabolism.<sup>10</sup> Moreover, decreased HSPG activity has been observed to lead to a greater number of mitochondria and fewer and smaller liposomes in larval fat body cells.<sup>3</sup>

The downregulation of HS biosynthetic enzymes in *Drosophila* has been achieved by lowering expression of *sulfateless* (*sfl*), a homolog of *NDST1*. *Sfl* controls the sulfation level of HS, and knocking down its activity decreases the sulfation on HS and has been seen to have effects on *Drosophila* that counteract what is observed in AD flies.<sup>3</sup> Because of this, we wanted to see what would happen when the downregulation of *Psn* and *sfl* were combined in a double knockdown model. These experiments utilized two models of *sfl* knockdowns: *sfl*<sup>RNAi</sup>, which reduces the amount of mRNA for *sfl* by 30-40%, and *sfl*<sup>03844</sup>, which is a null allele that reduces the amount of mRNA by about 50%. Due to it being a null allele, homozygosity for *sfl*<sup>03844</sup> is lethal, so any living fly with this genotype contains one copy of the *sfl*<sup>03844</sup> allele. Therefore, the total mRNA in a *sfl*<sup>03844</sup> animal is 50% of the wildtype level when heterozygous.

## Screening for bosutinib as a treatment

Since we have been attempting to rescue our AD model in *Drosophila* by downregulating *sfl* expression, we have also been looking into drugs that have a similar effect. Bosutinib, a tyrosine kinase inhibitor that is currently FDA-approved to treat chronic myelogenous leukemia, has been studied as a potential treatment of AD by Dr. Ryan Weiss' lab at the University of Georgia. In his 2021 paper published in Nature, he describes a genome-wide CRISPR screen of A375 melanoma cells that was done to find molecules that selectively bind to HS and regulate its biosynthesis. His lab made a tagged version of *EXT1*, a gene that encodes for polymerases critical in the synthesis of HS chains<sup>11</sup>, at its endogenous locus using CRISPR CAS9 to look at protein levels.<sup>12</sup>

After creating tags for *EXT1*, they screened a library of FDA-approved drugs for those that altered the level of *EXT1* expression with minimal cytotoxicity, and they then tested antibodies to evaluate how much HS was on the cell surface. From this, bosutinib was found to decrease *EXT1* expression, decrease HS at the cell surface, increase the size and number of mitochondria in the cell, and decrease the amount of lipid in the cell,<sup>13</sup> which are all beneficial in terms of rescuing the diseased phenotype that is observed in AD. Bosutinib works as a receptor tyrosine kinase inhibitor. Receptor tyrosine kinases are enzymes that control the growth and division of cells; when they bind a growth factor, cell division is initiated.<sup>14</sup> As a receptor tyrosine kinase inhibitor, bosutinib prevents these bound growth factors and receptors from going into a signaling cascade that would prevent autophagy. Therefore, bosutinib aids in increasing autophagic flux. It has also been shown to decrease HS on the cell surface by lowering *EXT1* expression, but the level at which this regulation occurs is not yet fully understood. Since HS is a coreceptor for growth factors and tyrosine kinases are receptors for

them, it was predicted that similar results would be observed between knocking down *sfl* expression or by treating diseased flies with bosutinib.

### ***UAS-Gal4 System***

This series of experiments studied the fat body cells of *Drosophila* larvae. The larval fat body was targeted because it is the principle metabolic regulatory organ in these animals, and these cells are high in lipids. Because we believe that AD is largely rooted in lipid metabolism, we wanted to study a part of the fly in which lipids are abundant. Targeting fat body also allows for good mitochondrial visualization, whose dysfunction is another main component of AD pathology. The results that have been observed in larval fat bodies are largely consistent with what we have seen in adult brains<sup>3</sup>, which is reassuring that fat body is a good target to study.

In order to localize AD pathology specifically in the fat body, the *UAS-Gal4* system was utilized. The *UAS-Gal4* system is a method of tissue-specific gene expression that uses two separate genotype lines. One line is designed to express *Gal4* in a specific tissue, and the other line carries a genetic construct where a gene of interest is expressed when the tissue-specific *Gal4* binds to its upstream activation sequence (*UAS*). As a result, when these two fly lines are crossed, *Gal4* expresses the desired gene in the particular tissue. This experiment crossed *R4-Gal4* flies, *R4* being a fat body target, with the various RNAi or mutated lines so that the knockdown of interest would occur within the fat body tissue. This meant that any effects from the knockdowns *Psn3<sup>RNAi</sup>*, *sfl<sup>RNAi</sup>*, and *sfl<sup>03844</sup>* or the double knockdowns *Psn3<sup>RNAi</sup>;sfl<sup>RNAi</sup>* and *Psn3<sup>RNAi</sup>;sfl<sup>03844</sup>* would be observed within the fat body. The Selleck Lab has also utilized *elav-gal4* flies in the past, which targets gene expression in neurons. In this model, knocking down

*Psn* has led to increased neuronal death<sup>3</sup>, which is consistent with what would be expected in an AD model. The figure below depicts a basic overview of the relationship between the *UAS-Gal4* system and RNAi.

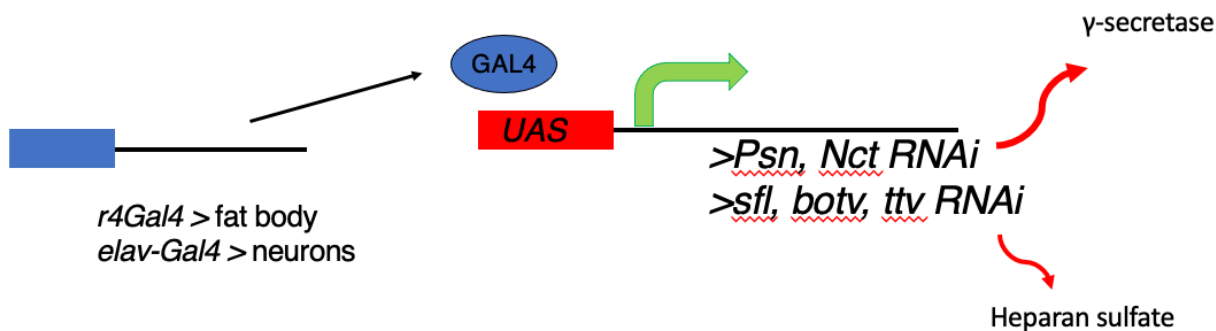


**Figure 3. Relationship between UAS-Gal4 and RNAi**

On the left of the figure, the blue rectangle represents a tissue-specific regulatory region, and the black line connected to it represents the coding sequence for transcriptional regulation of *Gal4*. It can be seen that *Gal4* is present in specific tissues, but it is only expressed in that tissue once it is activated by the *UAS*. Once crossed to the line containing the *UAS* RNAi, the respective gene is knocked down within that tissue. On the right, it is shown that *Psn* is related to changes in  $\gamma$ -secretase, and *sfl* is related to changes in HS.

## Chapter 2

### Materials and methods

#### Experimental design

Two main experiments were conducted in this study: the impact of *Psn* and *sfl* knockdown on fat body mitochondria and lipids and the impact of bosutinib treatment on fat body mitochondria and lipids. *UAS-w<sup>RNAi</sup>* acted as the wildtype control in every experiment since this is an RNAi construct that simply controls for eye color and as such has no effect on cell metabolism. The general approach of each experiment was to have an untreated control, a rescue model prior to its introduction to the AD model, an untreated AD model, and a treated AD model. This meant that for the double knockdown experiments, *w<sup>RNAi</sup>* was used as the control, *sfl<sup>03844</sup>* knockdown or *sfl<sup>RNAi</sup>* was observed to measure its initial impact, *UAS-Psn3<sup>RNAi</sup>* was used as the AD model, and *Psn3<sup>RNAi</sup>;sfl<sup>03844/RNAi</sup>* was used to measure the level of rescue in the AD model. *sfl<sup>03844</sup>* served as the rescue in the mitochondrial assessments, and *sfl<sup>RNAi</sup>* served as the rescue in the lipid assessments. This difference in *sfl* is simply because *sfl<sup>RNAi</sup>* was tested in lipids to remain consistent with the RNAi method, but since a mitochondrial rescue mediated by *sfl<sup>RNAi</sup>* has already been demonstrated in the Selleck Lab<sup>3</sup>, we tested the more drastic knockdown this time, which is *sfl<sup>03844</sup>*. Any flies observed with *sfl<sup>03844</sup>* knockdown were heterozygous for this allele due to it being a null allele and therefore lethal when homozygous. Males of each of these strains were crossed with *UAS-GFP-Atg8a; R4-Gal4* virgin females, and third instar larvae of each of these crosses were obtained for fat body dissection and imaging.

In the double knockdown experiments, flies were raised on standard food, and males of the four genotypes described above were crossed with *UAS-GFP-Atg8a*; *R4-Gal4* virgin females, which means that when crossed, larvae exhibit the gene knockdown effect in their fat bodies. Wandering third instar larvae offspring were acquired for dissection and imaging. The full crosses are shown below:

(female) *UAS-GFP-Atg8a*; *R4-Gal4*

X

(male) *UAS-w<sup>RNAi</sup>*

(female) *UAS-GFP-Atg8a*; *R4-Gal4*

X

(male) *UAS-shPsn3*

(female) *UAS-GFP-Atg8a*; *R4-Gal4*

X

(male) *sfl<sup>03844</sup>*

(female) *UAS-GFP-Atg8a*; *R4-Gal4*

X

(male) *shPsn3*; *sfl<sup>03844</sup>*

In the bosutinib treatment experiments, flies were raised on food containing either dimethyl sulfoxide (DMSO) or bosutinib dissolved in DMSO. DMSO is a widely used organic solvent that is miscible with many organic and inorganic substances. Bosutinib dissolves best in DMSO, but because DMSO is slightly toxic, the control food also contained DMSO to eliminate any negative confounding effects that DMSO might have had on the flies treated with bosutinib. Two genotypes were tested: *w*<sup>RNAi</sup> on both DMSO and bosutinib and *Psn3*<sup>RNAi</sup> on both DMSO and bosutinib. The full crosses are shown below:

(female) *UAS-GFP-Atg8a; R4-Gal4*

X

(male) *UAS-w*<sup>RNAi</sup>

(female) *UAS-GFP-Atg8a; R4-Gal4*

X

(male) *UAS-shPsn3*

### ***Drosophila* husbandry**

For the double knockdown experiments, fly strains were raised on standard cornmeal/sucrose/agar media at 25°C under a 12-hour day/12-hour night cycle. For the drug treatment experiments, fly strains were raised on standard cornmeal/sucrose/agar media with either 25% DMSO or 5 µM bosutinib dissolved in 25% DMSO added. They were raised under the same 25°C and 12-hour day/12-hour night cycle conditions. *UAS-w*<sup>RNAi</sup> flies served as a

wildtype control stock in each experiment, and they were obtained from Vienna Drosophila Resource Center (VDRC): *UAS-w<sup>RNAi</sup>* (VDRC#30033). *Sfl* strains were obtained from Bloomington Drosophila Stock Center (BDSC): *sfl<sup>03844</sup>* (BDSC#5575) and *UAS-sfl<sup>RNAi</sup>* (BDSC#34601). *UAS-shPsn3* was a generous gift from J. Kang at Harvard University. *UAS-GFP-Atg8a*; *R4-Gal4* flies were generated in the lab by Dr. Claire Reynolds-Peterson,<sup>10</sup> and *shPsn3*; *sfl<sup>03844</sup>* flies were generated in the lab by former undergraduate student Alex Kapral.

### Preparation of bosutinib in food

First, standard food making protocol was begun. 47 g agar, 517 g dextrose, 155 g brewer's yeast, 259 g sucrose, 858 g cornmeal, and 8.75 L cold tap water were combined in a cauldron and heated with steam until a temperature of 95°C was reached. After hitting this temperature, the steam was turned off, and the mixture was allowed to cool to 80°C. Once reaching 80°C, 113 mL Tegosept mix created from 190 g Tegosept powder dissolved in 736 mL 100% ethanol (Tegosept powder obtained from Apex Chemicals and Reagents, Cat# 20-258) and 100 mL acid mix (42% propionic acid/40% phosphoric acid/54% distilled water) were added and combined. Propionic acid was obtained from Sigma-Aldrich (Cas# 79-09-4), and phosphoric acid was obtained from EMD Millipore (Cas# 7664-38-2).

2 mL of ≥99.9% DMSO (obtained from ThermoFisher Scientific, Cat# 036480.K2) were added to 0.5 mL of 10 mM bosutinib (obtained from APExBIO, Cat# A2149), yielding a concentration of 2 mM bosutinib. 997.5 mL of the prepared food mixture were removed from the cauldron at a time and allowed to further cool to 60°C. Once cooled, the drug mixture was added

to generate a final result of 25% DMSO and 5  $\mu$ M bosutinib. DMSO control food consisted of 25% DMSO.

### **MitoTracker™ Red staining of fat bodies**

Wandering third instar larvae were collected and dissected in phosphate buffered saline solution (PBS). The purpose of dissection was to isolate the fat bodies so that the mitochondria in this tissue-specific target could be stained. Due to the ease of handling larvae, euthanization prior to dissection was not required. After dissection, fat bodies were transferred to a 100 nM solution of MitoTracker™ Red CMXRos (obtained from ThermoFisher Scientific, Cat# M7512). Fat bodies were incubated for thirty minutes at room temperature out of light, which was achieved by covering the wells that contained them with a piece of aluminum foil. The fat bodies were then washed in PBS, after which they were fixed in a 4% paraformaldehyde (PFA) solution and incubated for another thirty minutes at room temperature out of light. After incubation, they were again washed in PBS and transferred to a glass imaging slide containing ProLong™ Gold Antifade Mountant with DNA Stain DAPI (obtained from ThermoFisher Scientific, Cat# P36941) as a mounting medium with counterstain.

### **LipidTox™ Red staining of fat bodies**

Wandering third instar larvae were dissected in PBS and fixed in a 4% PFA solution. They were incubated for thirty minutes at room temperature out of light. After fixation, the fat bodies were washed in PBS. They were then transferred to a LipidTox™ Red neutral lipid staining solution (obtained from ThermoFisher Scientific, Cat# H34476) diluted 1:999 in PBS

and incubated for thirty minutes at room temperature out of light. Fat bodies were transferred to a glass imaging slide containing ProLong™ Gold Antifade Mountant with DNA Stain DAPI as a mounting medium with counterstain.

### **Confocal microscopy**

Images were captured at room temperature using an Olympus Fluoview FV3000 laser-scanning confocal microscope. Imaging was done on the same day that dissection and staining occurred to keep tissue degradation and signal loss to a minimum. Image capture settings were kept standard during mitochondrial imaging to ensure that any intensity differences observed in the samples were mostly due to actual differences in mitochondria signal and not because of laser settings. Image capture settings of lipids, however, were adjusted for each sample depending on how much laser intensity was required to best visualize the samples. Therefore, lipid analysis was mostly focused on morphology and not on signal intensity. All images were taken at 40X magnification. Mitochondria images are presented as maximum intensity projection Z-stacks spanning the depth of tissue where nuclei were observed, and lipid images are presented as individual slices of the tissue where nuclei were most prominent. All images were generated using Fiji ImageJ software.

### **Statistical analysis**

The signal intensity of mitochondria between samples was statistically analyzed through Kolmogorov Smirnov tests using Minitab with each sample being compared to the  $w^{\text{RNAi}}$  control. The data on average number of pixels per intensity level were gathered to create line graphs

depicting the distribution of signal for each sample, and these values were compared to p-values of 0.05, 0.01, and 0.001 to test for levels of significance.

No statistical analysis was done on lipids since different laser intensities were used to capture the images. These experiments were meant to gather information on lipid morphology differences rather than comparing differences in signal intensity.

## Chapter 3

### Results

#### ***Sfl*<sup>03844</sup> knockdown rescues *Psn3*<sup>RNAi</sup>-mediated abnormalities in mitochondria**

To determine whether introducing a *sfl* knockdown to fat body resulted in mitochondrial changes, fat body mitochondria of *w*<sup>RNAi</sup>, *sfl*<sup>03844</sup>, *Psn3*<sup>RNAi</sup>, and *sfl*<sup>03844</sup>;*Psn3*<sup>RNAi</sup> animals were stained and imaged, and differences in mitochondrial amount, size, and intensity between the four genotypes were observed. *W*<sup>RNAi</sup> animals, the control, appeared to have large mitochondria and mitochondrial density and intensity levels that were intermediate to those of *sfl*<sup>03844</sup> and *Psn3*<sup>RNAi</sup> animals. *Sfl*<sup>03844</sup> animals yielded mitochondria with the greatest density and most intense signal. *Psn3*<sup>RNAi</sup> animals yielded sparse, small mitochondria with very low signal intensity. Finally, *sfl*<sup>03844</sup>;*Psn3*<sup>RNAi</sup> animals, the double knockdown, resulted in cells densely packed with mitochondria with average signal intensity greater than the *w*<sup>RNAi</sup> animals. The mitochondria were slightly smaller in size than *w*<sup>RNAi</sup>, but in terms of amount and intensity, the *sfl* rescue drastically rescued the diseased phenotype. Kolmogorov Smirnov tests revealed a statistically significant difference in intensity levels between *sfl*<sup>03844</sup>, *Psn3*<sup>RNAi</sup>, and *sfl*<sup>03844</sup>;*Psn3*<sup>RNAi</sup> all compared to *w*<sup>RNAi</sup>. These results can be observed in the figures below.

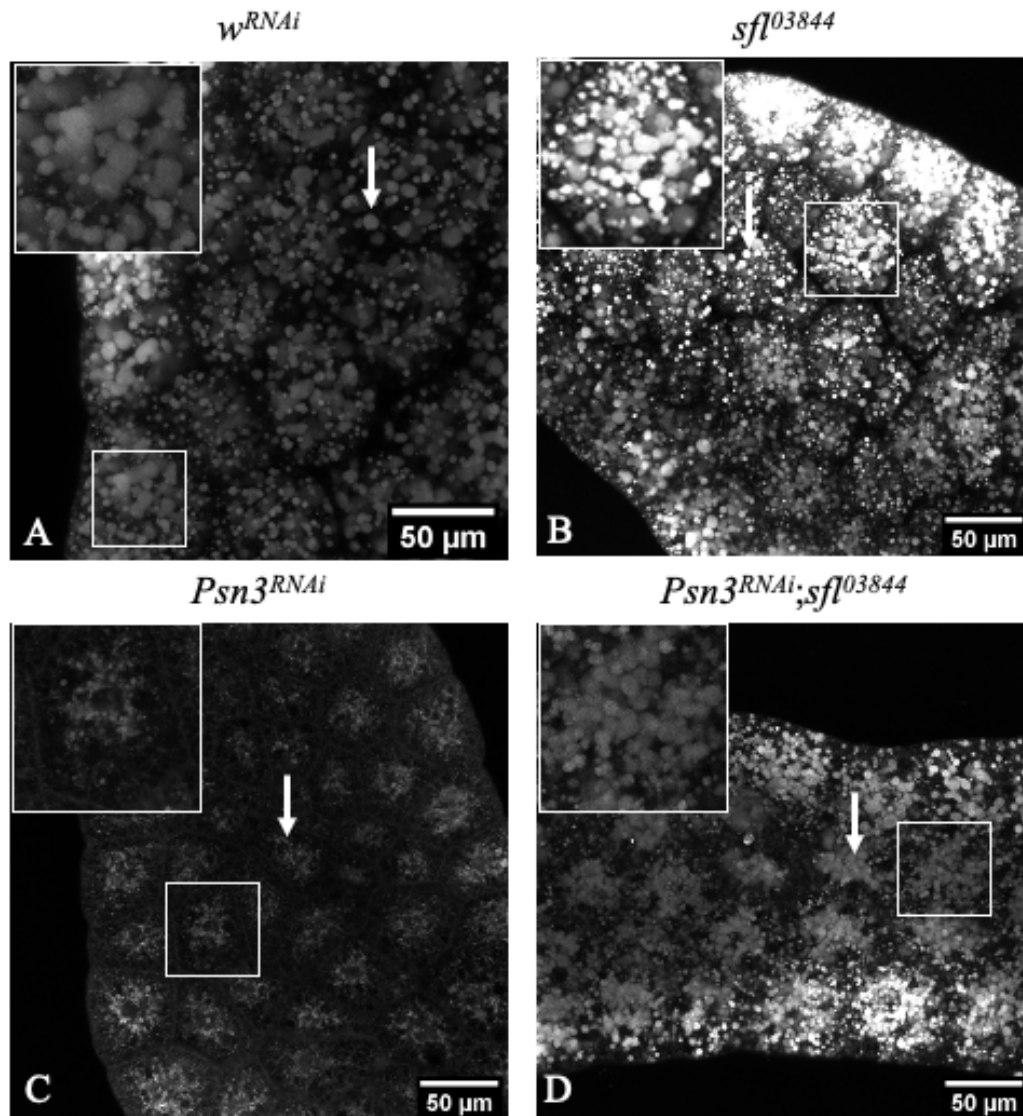


**Figure 4. *Psn3*<sup>RNAi</sup> and *sfl*<sup>03844</sup> downregulation alter mitochondrial number and morphology in fat body cells and double knockdown suppresses *Psn3*<sup>RNAi</sup>-induced changes**

Mitochondria are stained with MitoTracker™ Red and visualized by confocal serial selection. Images are maximum intensity projection Z-stacks depicting the organization and size of mitochondria. White arrows mark individual mitochondria, and white boxes indicate representative areas of the sample, which are magnified in the upper left corner of each image. Spheroid-shaped areas lacking signal are liposomes. (A) *w*<sup>RNAi</sup> control images depict wildtype mitochondrial organization and morphology. (B) *sfl*<sup>03844</sup> knockdown yields greater MitoTracker™ Red signal. (C) *Psn3*<sup>RNAi</sup> knockdown significantly reduces the amount of MitoTracker™ signal, and (D) *Psn3*<sup>RNAi</sup>;*sfl*<sup>03844</sup> yields mitochondria similar to those observed in

$w^{RNAi}$  and  $sfl^{03844}$  on its own, providing evidence that this double knockdown effectively suppresses the adverse impacts of  $Psn3^{RNAi}$  knockdown.

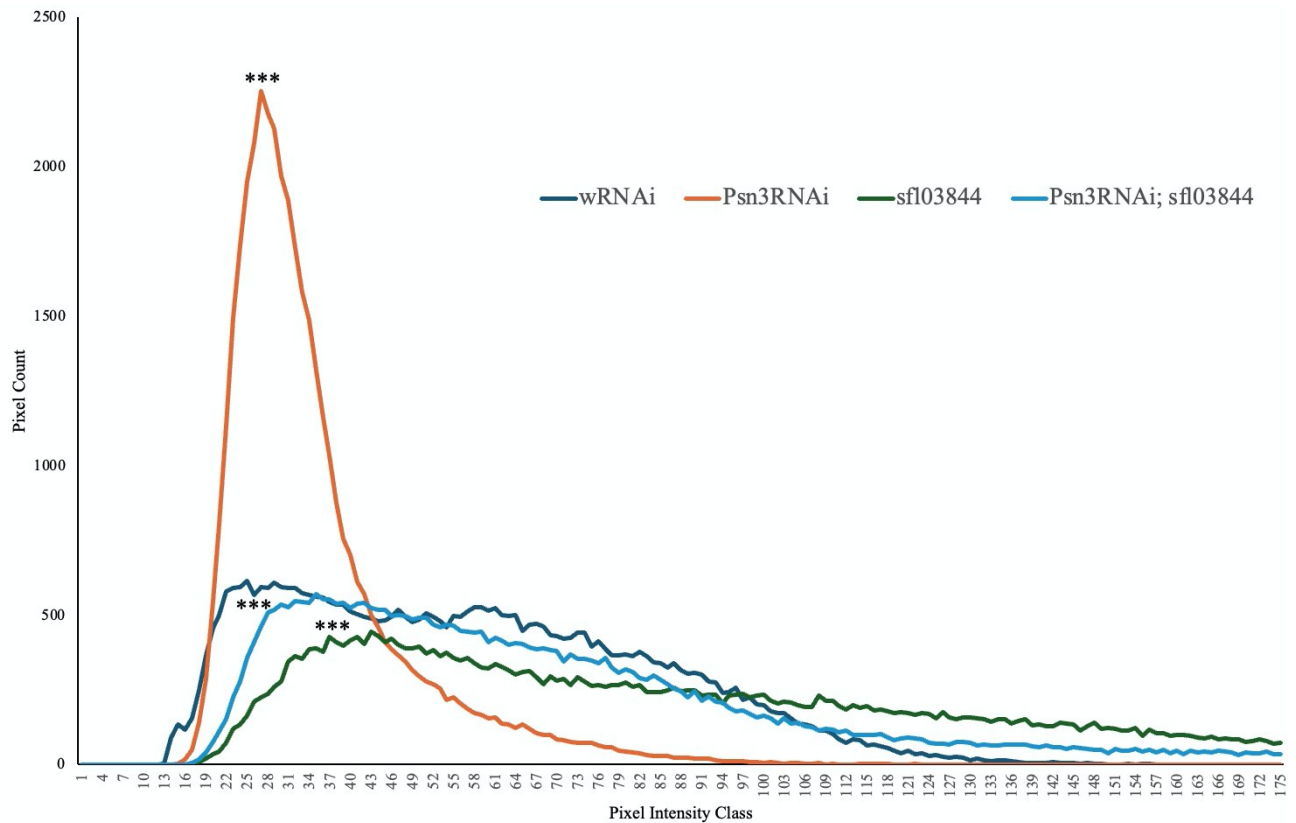


**Figure 5. Line graph of MitoTracker™ Red intensity distribution in *Drosophila* fat body cells with knockdown of  $sfl^{03844}$ ,  $Psn3^{RNAi}$ , or  $Psn3^{RNAi};sfl^{03844}$**

This graph shows the level of MitoTracker™ Red pixel intensity versus the number of pixels found at each intensity. Pixel intensities were taken as averages between 3 sections of a field per genotype. Knockdown of  $Psn3^{RNAi}$  significantly decreases the average pixel intensity of mitochondria compared to  $w^{RNAi}$  control, while knockdown of  $sfl^{03844}$  and  $Psn3^{RNAi};sfl^{03844}$  significantly increases the pixel intensity compared to  $w^{RNAi}$  control. (Kolmogorov-Smirnov test, \*\*\* $p < 0.001$ ).

### **Treatment with bosutinib rescues *Psn3*<sup>RNAi</sup>-mediated abnormalities in mitochondria**

Treatment of diseased flies with bosutinib yielded results similar to those achieved by *sfl*<sup>03844</sup> knockdown but to a more modest degree. *w*<sup>RNAi</sup> animals on both DMSO and bosutinib resulted in wildtype mitochondria that were densely packed within the cells and of moderate size. Treatment of *w*<sup>RNAi</sup> animals with bosutinib resulted in more mitochondrial signal of very high intensity than *w*<sup>RNAi</sup> animals on DMSO. *Psn3*<sup>RNAi</sup> animals on DMSO, the untreated group, showed significantly less MitoTracker™ Red signal than in *w*<sup>RNAi</sup> animals, but when treated with bosutinib, the mitochondria significantly increased in intensity and appeared to be larger and more densely packed within the cells. The mitochondria observed in the treated diseased state appear to be more similar to those of the control than those of just the diseased state on its own, but *Psn* knockdown mitochondria still had a lower average signal intensity than *w*<sup>RNAi</sup>, indicating that *sfl* knockdown was a more effective rescue. Kolmogorov Smirnov tests revealed a statistically significant difference in intensity levels between *w*<sup>RNAi</sup> on bosutinib, *Psn3*<sup>RNAi</sup> on DMSO, and *Psn3*<sup>RNAi</sup> on bosutinib all compared to the control, *w*<sup>RNAi</sup> on DMSO. These results can be observed in the figures below.

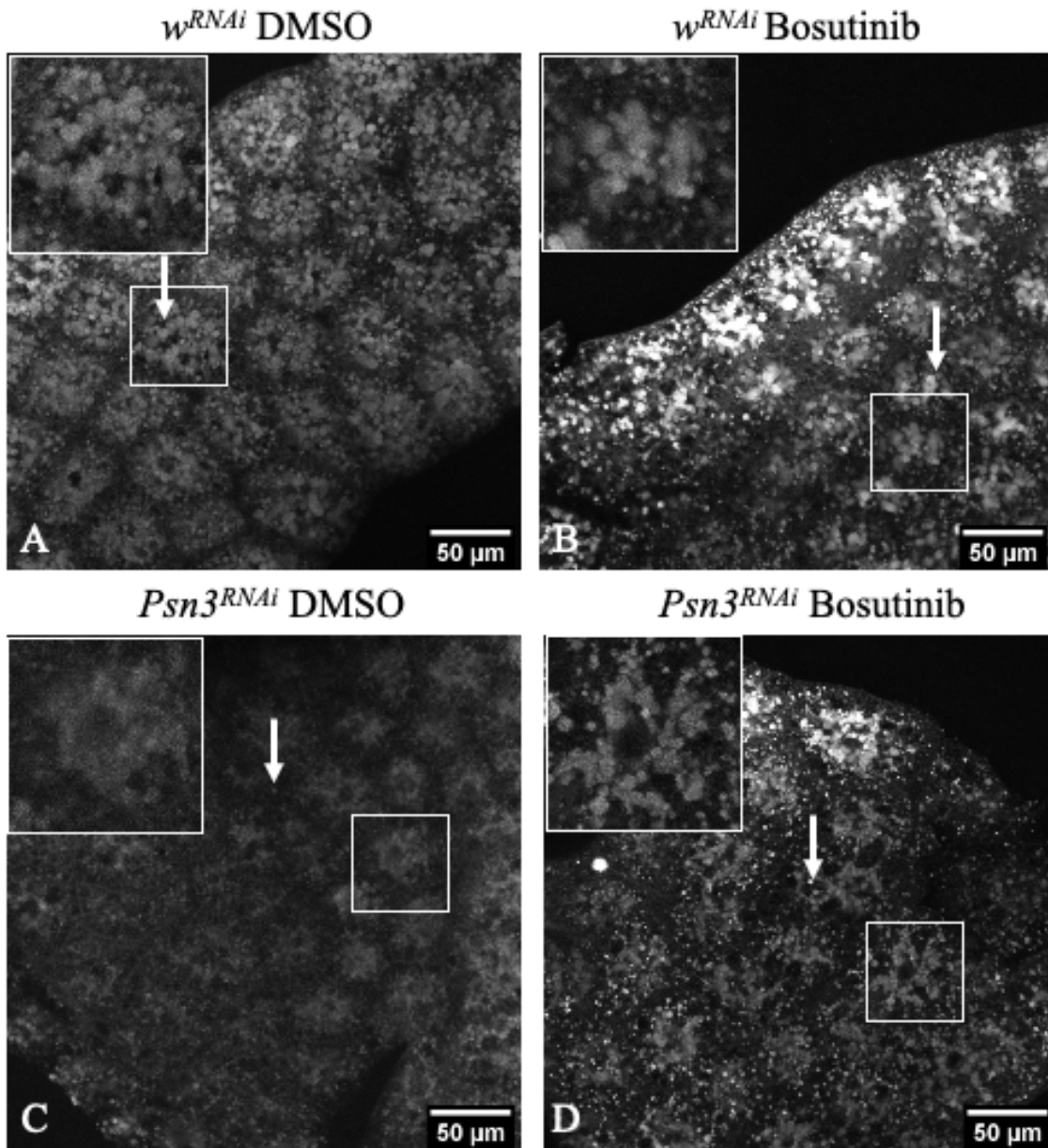


**Figure 6. *Psn3*<sup>RNAi</sup> alters mitochondrial number and morphology in fat body cells and treatment with bosutinib suppresses *Psn3*<sup>RNAi</sup>-induced changes**

Mitochondria are stained with MitoTracker™ Red and visualized by confocal serial selection. Images are maximum intensity projection Z-stacks depicting the organization and size of mitochondria. White arrows mark individual mitochondria, and white boxes indicate representative areas of the sample, which are magnified in the upper left corner of each image. Spheroid-shaped areas lacking signal are liposomes. (A) *w*<sup>RNAi</sup> on DMSO depicts wildtype mitochondrial organization and morphology. (B) *w*<sup>RNAi</sup> on bosutinib again depicts wildtype organization with greater signal. (C) *Psn3*<sup>RNAi</sup> knockdown significantly reduces the amount of

MitoTracker™ signal, and (D) treatment of it with bosutinib yields mitochondria similar to those observed in  $w^{RNAi}$ , effectively suppressing the adverse impacts of  $Psn3^{RNAi}$  knockdown.

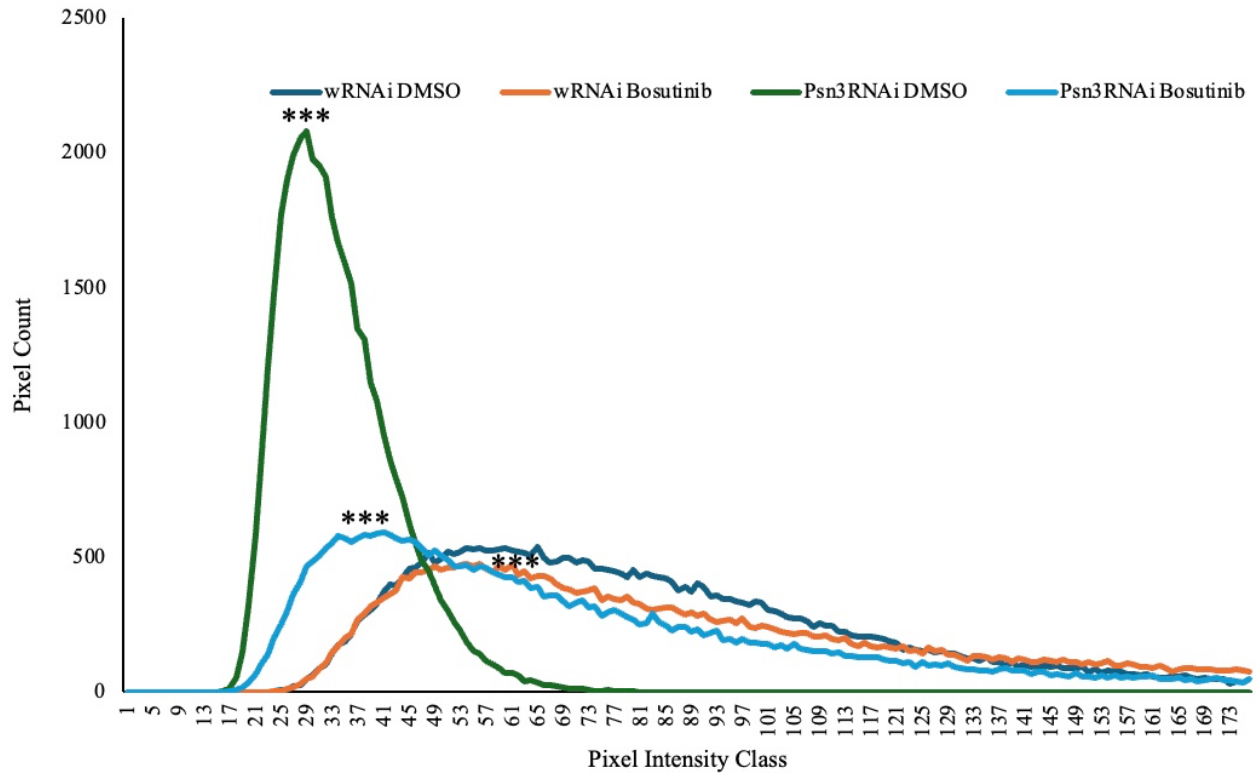


**Figure 7. Line graph of MitoTracker™ Red intensity distribution in *Drosophila* fat body cells treated with bosutinib**

This graph shows the level of MitoTracker™ Red pixel intensity versus the number of pixels found at each intensity. Pixel intensities were taken as averages between 3 sections of a field per genotype. Knockdown of  $Psn3^{RNAi}$  significantly decreases the average pixel intensity of mitochondria compared to  $w^{RNAi}$ , while treatment of  $Psn3^{RNAi}$  with bosutinib increases the average pixel intensity.  $w^{RNAi}$  on DMSO is still significantly greater in intensity than  $Psn3^{RNAi}$  on bosutinib (Kolmogorov-Smirnov test, \*\*\* $p < 0.001$ ).

### ***Sft*<sup>RNAi</sup> impacts *Psn3*<sup>RNAi</sup>-mediated alterations in liposome morphology**

Liposome morphology was evaluated by confocal microscopy of neutral lipid fluorophore staining (LipidTox™ Red). *W*<sup>RNAi</sup> control animals show round, regular liposomes that mostly fill the entire cell. *Sft*<sup>RNAi</sup> animals yield sparser, smaller liposomes than the control, indicating an increase in lipophagy. *Psn3*<sup>RNAi</sup> animals have large, irregularly shaped liposomes that do not have clear borders like those in the *w*<sup>RNAi</sup> animals, indicating both the fusion of some of the liposomes and the presence of lipid in parts of the cell outside of the liposomes. In addition to these irregularly shaped liposomes, *Psn3*<sup>RNAi</sup> animals show smaller spherical structures that lack signal, which are not observed in the *w*<sup>RNAi</sup> nor *sft*<sup>RNAi</sup> animals. These smaller structures are autophagosome-related organelles, and this was confirmed in past experiments conducted by the Selleck Lab. In these experiments, fat bodies were stained with GFP-Atg8a, which is an autophagosome marker. Upon imaging, these organelles were found to be Atg8a-positive, indicating that they are autophagosome-related.<sup>3</sup> The presence of these autophagy intermediates in *Psn3*<sup>RNAi</sup> animals is evidence of an interruption in the normal autophagy process in the AD model. Lastly, while *Psn3*<sup>RNAi</sup>;*sft*<sup>RNAi</sup> animals still show some signal-lacking autophagosome-related organelles, they are fewer in number than in the *Psn* knockdown animals. The liposomes appear rounder in morphology with more distinct borders, indicating that lipids are confined to the liposomes unlike in the *Psn3*<sup>RNAi</sup> animals. These results can be observed in the figure below.

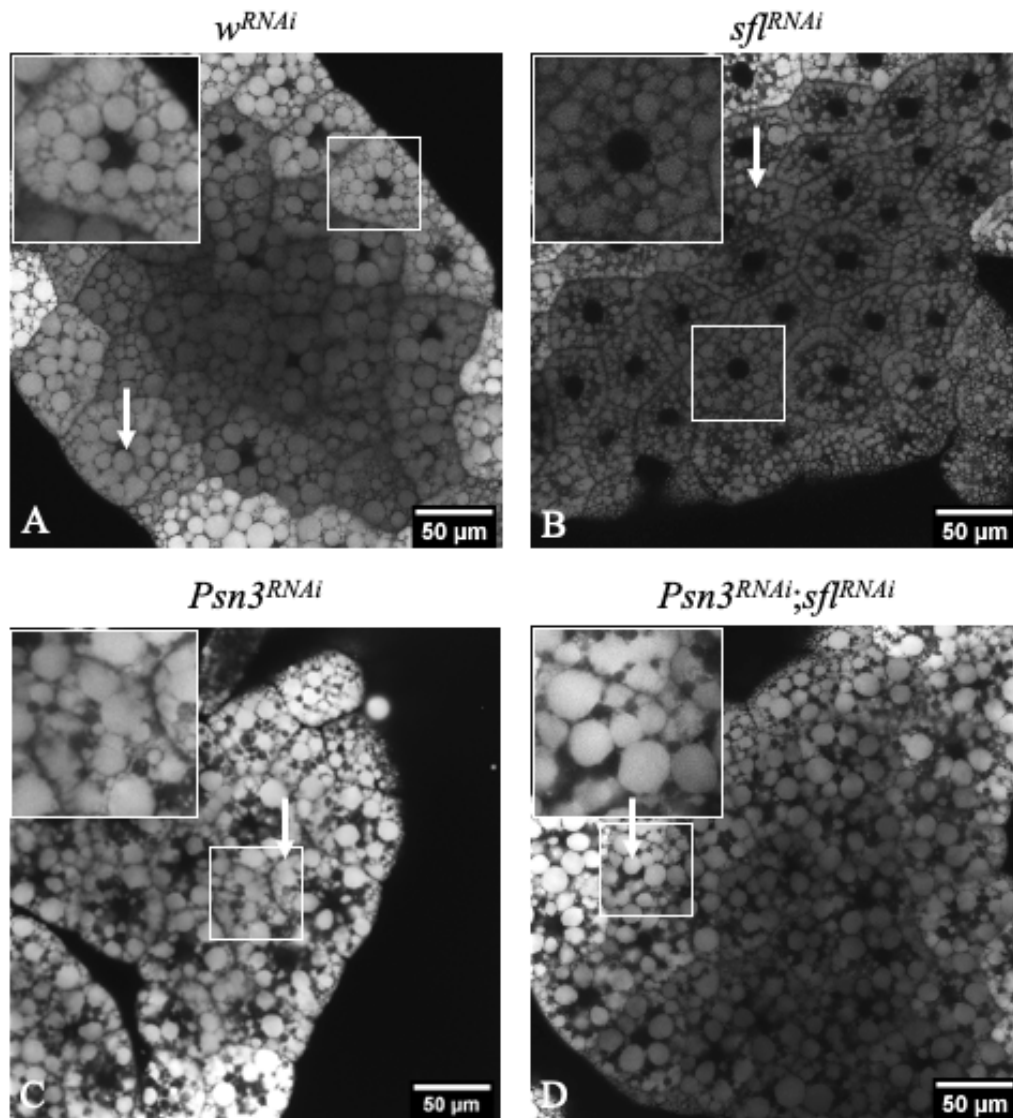


**Figure 8. *Sfl*<sup>RNAi</sup> partially reverts *Psn3*<sup>RNAi</sup>-mediated changes in liposome morphology**

Liposomes are stained with LipidTox™ Red and visualized by confocal serial selection. Images are individual slices of the sample depicting the organization and size of liposomes. White arrows mark individual liposomes, and white boxes indicate representative areas of the sample, which are magnified in the upper left corner of each image. Small spheroid-shaped areas lacking signal are autophagosome-related organelles, and large areas lacking signal in the central region of cells are nuclei. (A) *w*<sup>RNAi</sup> control images depict wildtype liposome organization and morphology. (B) *sfl*<sup>03844</sup> knockdown yields smaller and less dense liposomes. (C) *Psn3*<sup>RNAi</sup> knockdown leads to amorphous liposomes and the presence of autophagosomes, and (D) *Psn3*<sup>RNAi</sup>;*sfl*<sup>03844</sup> yields fewer autophagosomes and more regularly-shaped liposomes. The images used in this figure were taken by Sophia DeGuara, an undergraduate in the Selleck Lab.

### **Treatment with bosutinib impacts *Psn3*<sup>RNAi</sup>-mediated alterations in liposome morphology**

Treatment of *Psn* knockdown animals with bosutinib appeared to have effects on liposome morphology, but more data must be gathered to determine just how much of an impact it has. Liposome morphology was again evaluated by confocal microscopy of neutral lipid fluorophore staining (LipidTox™ Red). *W*<sup>RNAi</sup> animals on DMSO and bosutinib display liposomes of similar appearance; they are round and have fairly distinct borders. Those treated with bosutinib appear to have greater variation in size, but the significance of this is unknown. *Psn3*<sup>RNAi</sup> animals show cells with more densely packed liposomes, and like in the previous lipid experiment, the liposome borders on this AD model are less distinct, indicating the possible presence of lipid outside of the liposomes. Treatment of this diseased model with bosutinib results in more well-defined liposomes that are less densely packed within the cells than the untreated ones, which could indicate more efficient lipid metabolism in these treated cells. These results can be observed in the figure below.

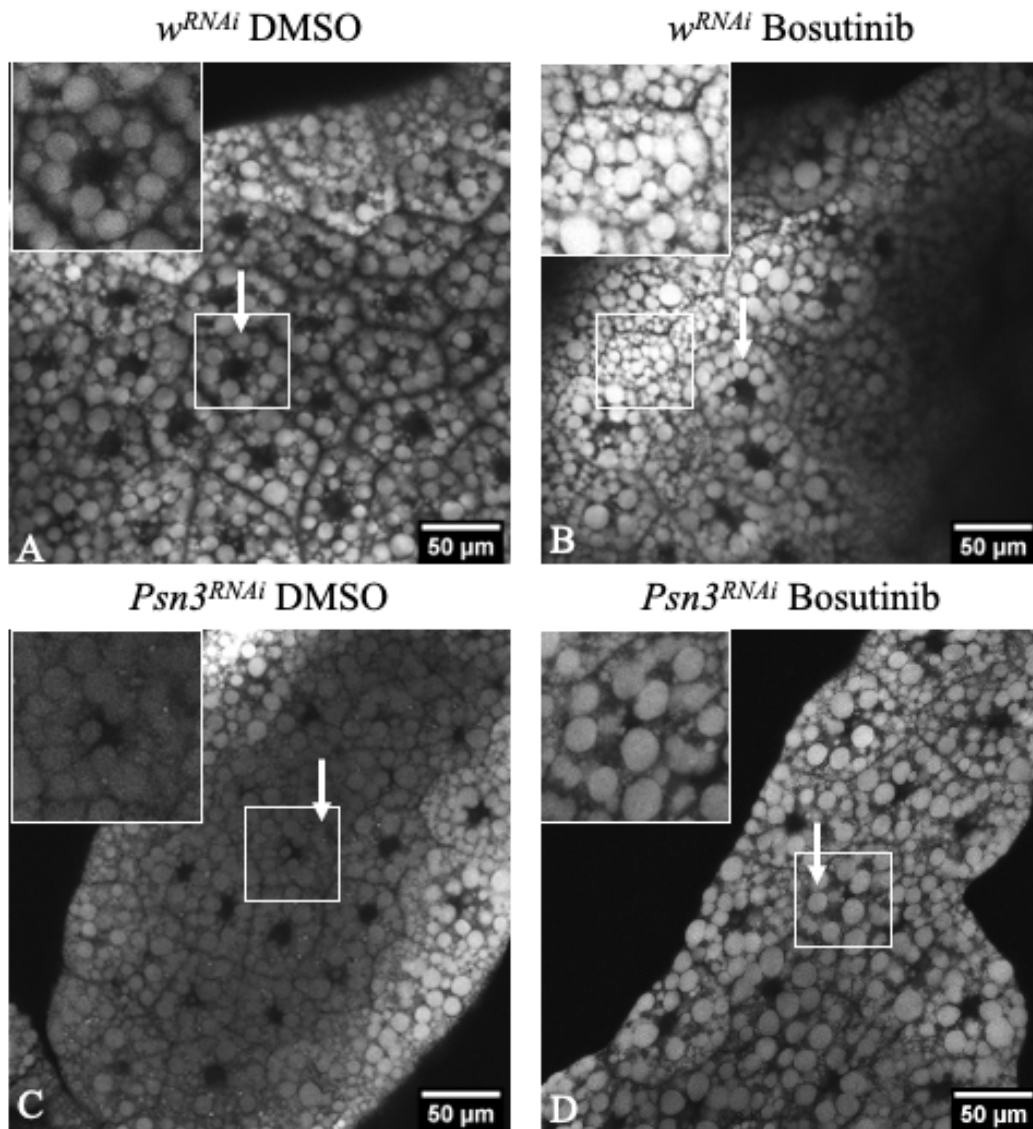


**Figure 9. Treatment with bosutinib partially reverts  $Psn3^{RNAi}$ -mediated changes in liposome morphology**

Liposomes are stained with LipidTox™ Red and visualized by confocal serial selection. Images are individual slices of the sample depicting the organization and size of liposomes. White arrows mark individual liposomes, and white boxes indicate representative areas of the sample, which are magnified in the upper left corner of each image. Large areas lacking signal in the central region of cells are nuclei. (A)  $w^{RNAi}$  on DMSO and (B)  $w^{RNAi}$  on bosutinib control images depict wildtype liposome organization and morphology. (C)  $Psn3^{RNAi}$  knockdown leads to densely packed, amorphous liposomes, and (D)  $Psn3^{RNAi}$  treated with bosutinib yields less dense, regularly-shaped liposomes.

## Chapter 4

### Discussion

#### **Dysfunction of mitochondria and lipid metabolism are implicated in AD**

In this study, an AD model was induced in *Drosophila* by knocking down *Psn*. *PSEN1* plays a large role in autophagy, and mutations in it are known to be one of the main determinants of early-onset AD in humans. Reducing *Psn* function in larval fat bodies led to fewer, smaller mitochondria and decreased signal as well as irregular liposome morphology. Since it is already known that *PSEN1* downregulation in humans is the main determinant of AD onset and these are the impacts of its reduction in function that are observed in *Drosophila*, this suggests that AD is a disease of cellular metabolism dysfunction at its core. If autophagy cannot be carried out properly, damaged mitochondria and liposomes are not able to be degraded via mitophagy and lipophagy, and this is what contributes to the characteristics that are observed in AD. This explains why past attempts at treating AD that have solely focused on  $\beta$ -amyloid plaque accumulation have not been very successful. Instead, focusing on increasing autophagy and improving mitochondria and lipid metabolism as the primary targets of AD treatment may be more successful.

The rationale as to why fewer mitochondria are observed in the *Psn* model if autophagic flux is decreased in these animals could be for a multitude of reasons. The overarching idea, though, is that the mitochondria present in the *Psn* knockdown fat bodies are damaged, while those in the rescued fat bodies are healthier. A paper written by Ju and colleagues (2016)

explains how mitochondrial homeostasis is regulated by mitochondrial biogenesis and mitophagy. In their study, inducing an increase in autophagic flux in mouse skeletal muscle through cardiovascular exercise led to increases in mitochondrial biogenesis promoting factors and mitochondrial biogenesis marker proteins.<sup>15</sup> These findings apply to our research because by increasing autophagy, damaged mitochondria are degraded, and the biogenesis of undamaged mitochondria is promoted. The generation of these undamaged mitochondria then aids in further autophagy of damaged cell components and increased lipophagy, which supports why rescued fat bodies show more mitochondria of greater size and less liposome density on average. Another study by Kang and colleagues (2018) found that loss-of-function *Psn* mutations downregulate important transcription factors of mitochondrial biogenesis<sup>16</sup>, which could be another cause of the decrease in number of mitochondria observed in *Psn* mutant animals. *Psn* mutations may also interfere with the regular fission/fusion cycle of mitochondria, which are the processes by which mitochondria divide into separate organelles or merge into one larger organelle. This could impact their number and size, resulting in the sparser and smaller mitochondria that we observe. Finally, more autophagy does not necessarily mean that fewer mitochondria should be observed because autophagy does not target healthy organelles. If the mitochondria in rescued animals are undamaged, then they will not be degraded even in the presence of a greater autophagic flux.

### **Decreasing heparan sulfate improves AD pathology**

As a coreceptor for growth factors and growth factor receptors, HSPGs are largely involved in the level of autophagy in cells. By decreasing HSPG biosynthesis, autophagy is increased, which promotes the removal of damaged mitochondria and lipid catabolism. When

paired with *Psn* downregulation, knocking down *sfl*, one of the biosynthetic enzymes of HS, leads to a reversal of the detrimental effects seen in *Psn* knockdown.

The effects of *sfl* knockdown in *Drosophila* fat body were observed by imaging the mitochondria and liposomes. While *Psn*<sup>3<sup>RNAi</sup> resulted in extremely low mitochondria signal, when paired with *sfl*<sup>03844</sup> knockdown, this signal increased significantly (**Fig. 4**). This is further demonstrated in **Fig. 5**, which shows the significant differences in mitochondria signal intensity between the four genotypes graphed. The vast majority of *Psn*<sup>3<sup>RNAi</sup> mitochondrial signal exists in the low intensity range, while *Psn*<sup>3<sup>RNAi</sup>;*sfl*<sup>03844</sup> mitochondrial signal is significantly more intense on average. Additionally, *Psn*<sup>3<sup>RNAi</sup> yielded amorphous liposomes and the buildup of autophagosome-related organelles, while the simultaneous knockdown of *sfl* resulted in a return of liposomes to their regular morphology and a lack of these autophagic intermediates (**Fig. 8**). This is consistent with what was expected since prior research has shown that *Psn* mutations lead to an increase in autophagic intermediates but a decrease in autophagy due to *Psn* being unable to properly bind lysosomes to autophagosomes and carry autophagy to completion.<sup>5</sup></sup></sup></sup></sup>

Snow and colleagues (2021) discovered similar results. These researchers propose that the underlying link between  $\beta$ -amyloid deposits, tau tangles, inflammation, and other symptoms of AD is HS accumulation. They explain that HS accumulation/decreased degradation induces tau protein to form tangles in the brain, and it also leads to the formation of plaques in the brain.<sup>17</sup> Therefore, rather than targeting these plaques themselves, there is evidence to suggest that instead, inducing autophagy through decreased HS could be more effective.

## Bosutinib as a potential treatment of AD

Consistent with our hypothesis that HSPG modification affects AD outcomes, we predicted that treating our AD model with bosutinib would yield similar results due to the prior discovery that it decreases HS at the cell surface in A375 melanoma cells.<sup>13</sup> Differences were again observed in both the mitochondria and liposomes of larval fat bodies. Similar to knocking down *sfl*, treating *Psn3<sup>RNAi</sup>* flies with bosutinib resulted in mitochondria of greater number, size, and intensity (**Fig. 6-7**). While the liposome results were not quite as conclusive, a difference in liposome morphology could still be observed to some extent between *Psn3<sup>RNAi</sup>* flies treated with bosutinib versus those left untreated. *Psn3<sup>RNAi</sup>* animals on DMSO showed cells densely packed with liposomes that varied in shape and had nondistinctive outlines, while *Psn3<sup>RNAi</sup>* animals on bosutinib showed cells with fewer liposomes that were rounder in shape and more distinct (**Fig. 9**). This is fairly consistent with what was observed in the double knockdown liposomes, but further replication and quantification need to be done to generate more conclusive results. Nevertheless, bosutinib still displayed rescue of the mitochondria in *Psn3<sup>RNAi</sup>* animals, so it might be promising in finding an effective treatment for AD in humans.

Although not too much investigation into the effect of bosutinib on AD pathology has been done yet, Mahdavi and colleagues (2021) have come to similar conclusions that we have regarding bosutinib. These Los Angeles researchers gathered 31 patients between the ages of 45 and 89 with probable Alzheimer's or Parkinson's disease and treated them with bosutinib for 12 months followed by 12 months of follow-up. There was no explicit control group in this study, which is common for clinical trials. Rather, Clinical Dementia Rating (CDR) scores of the participants were compared to population-based estimates of decline, which were calculated by averaging reported values in existing literature. These population-based estimates of decline

were an expected 22% progression rate from mild cognitive impairment (MCI) to dementia and a 29% progression rate to a more advanced stage of dementia. The estimates of improvement were 5.6% improvement for MCI and 0% for dementia. After only one year of treatment, just over 45% of the participants had an improved Clinical Dementia Rating (CDR) score, and another 45% had a stable CDR score. Only about 9% displayed a worsened CDR score. The main finding was that bosutinib treatment led to significantly less worsening in CDR scores compared to the population-based estimate of decline. Moreover, most of the participants experienced no negative side effects, which means that bosutinib is likely safe for most patients.<sup>18</sup> In this study, the maximum dosage of bosutinib given was only 300 mg, while those taking bosutinib for chronic myelogenous leukemia (CML) commonly take up to 500 mg.<sup>19</sup> This means that bosutinib as a treatment for AD would not even need to be given at as large of a dose as it is for CML, and it is still shown to be beneficial. In this study, after discontinuing bosutinib treatment, the patients resumed cognitive decline that would normally be observed in Alzheimer's and Parkinson's disease.<sup>18</sup> This further supports the idea that bosutinib can be used as an effective treatment against AD and potentially other neurodegenerative disorders as well.

### **Limitations**

The greatest limitation throughout this entire study was the number of replicates of each experiment. Each experiment was only conducted a few times due to time restraints, and with a low number of repetitions, we cannot be positive that these results are representative of all cases of *Psn3<sup>RNAi</sup>*-induced AD models in *Drosophila*. We can reasonably conclude that the results are representative based on what has previously been studied in Selleck Lab, but still, as these

experiments are carried out more, we can become increasingly confident that these are the results that are observed most often.

As far as LipidTox™ Red staining and imaging goes, different laser intensities were used to image each sample in order to best visualize the liposomes. Although this allowed us to best study morphological differences, signal intensity differences could not be quantified. In the future, if imaging settings are held constant, average lipid signal in each sample can be quantified and statistically analyzed to measure differences better mathematically between treatment groups like what was done in the mitochondria images. Furthermore, if statistical analysis of size and number of mitochondria and lipids is done in addition to signal intensity, a more comprehensive idea of mitochondria and lipid metabolism in AD can be understood.

For the bosutinib treatment experiments, only one bosutinib dosage, 5  $\mu$ M, was tested. Although this dosage did yield noticeable improvements in mitochondrial signal and changes in lipid morphology, the impact that bosutinib had on fat body cells was not as large as the impact of *sfl* knockdown. In the future, varying bosutinib doses should be tested to find the dosage at which the most beneficial effects are observed.

### **Future directions**

The effects of *Psn* and *sfl* knockdowns on *Drosophila* brains have largely been studied in the Selleck Lab. It has been previously found that *Psn*<sup>3<sup>RNAi</sup> increases the size and number of vacuoles in the brain, while introducing a simultaneous *sfl* knockdown suppresses these effects.<sup>3</sup> It would be interesting to see, though, how bosutinib treatment of *Psn*<sup>3<sup>RNAi</sup> animals affects vacuole formation in the brain since as of now, we have only researched its impacts on the larval</sup></sup>

fat body. Along with this, varying bosutinib dosages should be administered, and these different dosages should be studied through imaging of larval mitochondria and fat body as well as adult brains.

So far, we have studied the impact of bosutinib on our AD model since bosutinib is already FDA-approved for the treatment of chronic myelogenous leukemia, and in Ryan Weiss' lab, it has been shown to lower HS levels on the cell surface while imposing minimal cytotoxicity. In the future, though, it would be interesting to test additional receptor tyrosine kinase inhibitors besides bosutinib to see if any of them yield more significant results. Additionally, it would be helpful to screen for other classes of drugs entirely. More noticeable changes were observed when knocking down *sfl* as opposed to treating animals with bosutinib, and these two treatments operate under different mechanisms. HSPGs act as coreceptors for growth factors, while bosutinib is an inhibitor of growth factor receptors themselves. Even though they are both ultimately suppressing the activity of growth factors and leading to increased autophagic flux, I would be curious to see whether drugs that act under the same mechanism as HSPGs have a greater effect on AD pathology than bosutinib. This would mean testing drugs that directly lower the sulfation level of HS rather than those that operate under a different mechanism and just happen to decrease HS levels as a side effect like bosutinib.

Finally, future research could be done that measures the impact of *sfl* downregulation and drug treatment on other neurodegenerative disease models in addition to AD such as Parkinson's disease (PD) and amyotrophic lateral sclerosis (ALS). Mitochondrial dysfunction is implicated in both PD and ALS<sup>20,21</sup>, and the accumulation of lipids has been observed in models of these disorders as well.<sup>22,23</sup> Since these are the major hallmarks of AD that were studied in this paper, this suggests that multiple neurodegenerative disorders originate from the same metabolic issues.

The methods of improving mitochondria and lipid metabolism in AD were shown to be promising in these experiments, so I would be interested to see the results of these experiments in additional neurodegenerative disease models. This would also help us better understand the similarities in causes and development between these various disorders.

## Chapter 5

### Conclusion

Overall, *PSENI* and HSPGs are both shown to be major factors in AD onset and progression due to their impacts on cellular metabolism and autophagy. We were able to identify two potential rescues of AD in a *Drosophila* model: *sfl* downregulation and bosutinib treatment. While the *sfl* knockdown yielded stronger results than bosutinib, both are promising in identifying a future treatment for AD. With the results obtained from this study, we can further investigate the effects of these two rescues on AD pathology in other *Drosophila* pathways and expand our findings to better understand the nature of neurodegenerative disorders as a whole.

## BIBLIOGRAPHY

1. U.S. Department of Health and Human Services. (2023, April 5). *Alzheimer's disease fact sheet*. National Institute on Aging. <https://www.nia.nih.gov/health/alzheimers-and-dementia/alzheimers-disease-fact-sheet#:~:text=Alzheimer's%20disease%20is%20named%20after,language%20problems%2C%20and%20unpredictable%20behavior>
2. Parzych, K. R., & Klionsky, D. J. (2014a). An overview of autophagy: morphology, mechanism, and regulation. *Antioxidants & Redox Signaling*, *20*(3), 460–473. <https://doi.org/10.1089%2Fars.2013.5371>
3. Schultheis, N., Connell, A., Kapral, A., Becker, R. J., Mueller, R., Shah, S., O'Donnell, M., Roseman, M., Wang, W., Yin, F., Weiss, R., & Selleck, S. B. (2024, January 25). *Heparan sulfate modified proteins affect cellular processes central to neurodegeneration and modulate presenilin function*. bioRxiv. <https://www.biorxiv.org/content/10.1101/2024.01.23.576895v1.full.pdf>
4. Nakamura, S., & Yoshimori, T. (2018). *Overview of macroautophagy*. National Library of Medicine. National Center for Biotechnology Information.
5. Uddin, M. S., Stachowiak, A., Mamun, A. A., Tzvetkov, N. T., Takeda, S., Atanasov, A. G., Bergantin, L. B., Abdel-Daim, M. M., & Stankiewicz, A. M. (2018). Autophagy and Alzheimer's disease: from molecular mechanisms to therapeutic implications. *Frontiers in Aging Neuroscience*, *10*(4). <https://doi.org/10.3389%2Ffnagi.2018.00004>

6. Collins, M. P., & Forgac, M. (2021). Regulation and function of V-ATPases in physiology and disease. *Biochimica et Biophysica Acta (BBA) - Biomembranes*, 1862(12). <https://doi.org/10.1016%2Fj.bbamem.2020.183341>
7. Nature Education. (2014). *Hairpin loop (mRNA)*. Scitable by Nature Education. <https://www.nature.com/scitable/definition/hairpin-loop-mrna-314/>
8. Iozzo, R. V. (2001). Series introduction: Heparan sulfate proteoglycans: Intricate molecules with intriguing functions. *The Journal of Clinical Investigation*, 108(2), 165–167. <https://doi.org/10.1172%2FJCI13560>
9. Balagurunathan, K. (2024). *Heparan sulfate (HS) proteoglycan*. The University of Utah. The University of Utah. Retrieved from <https://neuroscience.med.utah.edu/faculty/balagurunathan.php>.
10. Reynolds, C. E., Zhao, N., Xu, J., Serman, T. M., & Selleck, S. B. (2017). Heparan sulfate proteoglycans regulate autophagy in *Drosophila*. *Autophagy*, 13(8), 1262–1279. <https://doi.org/10.1080/15548627.2017.1304867>
11. Okada, M., Nadanaka, S., Shoji, N., Tamura, J., & Kitagawa, H. (2010). Biosynthesis of heparan sulfate in EXT1-deficient cells. *Biochemical Journal*, 428(3), 463–471. <https://doi.org/10.1042/BJ20100101>
12. Weiss, R.J., Spahn, P.N., Chiang, A.W.T. *et al.* Genome-wide screens uncover KDM2B as a modifier of protein binding to heparan sulfate. *Nat Chem Biol* 17, 684–692 (2021). <https://doi.org/10.1038/s41589-021-00776-9>
13. Weiss, R. J. (2024). Research plan.

14. Hubbard, S. R., & Miller, W. T. (2007b). Receptor tyrosine kinases: mechanisms of activation and signaling. *Current Opinion in Cell Biology*, *19*(2), 117–123.  
<https://doi.org/10.1016%2Fj.ceb.2007.02.010>
15. Ju, Js., Jeon, Si., Park, Jy. *et al.* Autophagy plays a role in skeletal muscle mitochondrial biogenesis in an endurance exercise-trained condition. *J Physiol Sci* **66**, 417–430 (2016).  
<https://doi.org/10.1007/s12576-016-0440-9>
16. Kang, I., Chu, C. T., & Kaufman, B. A. (2018). The mitochondrial transcription factor TFAM in neurodegeneration: Emerging evidence and mechanisms. *FEBS Letters*, *592*(5), 793–811. <https://doi.org/10.1002%2F1873-3468.12989>
17. Snow AD, Cummings JA, Lake T. The Unifying Hypothesis of Alzheimer's Disease: Heparan Sulfate Proteoglycans/Glycosaminoglycans Are Key as First Hypothesized Over 30 Years Ago. *Frontiers in Aging Neuroscience*. 2021 Oct 4;13:710683. doi: 10.3389/fnagi.2021.710683. PMID: 34671250; PMCID: PMC8521200.
18. Mahdavi, K. D., Jordan, S. E., Barrows, H. R., Pravdic, M., Habelhah, B., Evans, N. E., Blades, R. B., Iovine, J. J., Becerra, S. A., Steiner, R. A., Chang, M., Kesari, S., Bystritsky, A., O'Connor, E., Gross, H., Pereles, F. S., Whitney, M., & Kuhn, T. (2021). Treatment of dementia with bosutinib. *Neurology Clinical Practice*, *11*(3), e294–e302.  
<https://doi.org/10.1212%2FCPJ.0000000000000918>
19. Isfort, S., Manz, K., Teichmann, L. L., Crysandt, M., Burchert, A., Hochhaus, A., Saussele, S., Kiani, A., Gothert, J. R., Illmer, T., Schafhausen, P., Al-Ali, H. K., Stegelmann, F., Hanel, M., Pfeiffer, T., Giagounidis, A., Franke, G.-N., Koschmieder, S., Fabarius, A., ... Brummendorf, T. H. (2023). Step-in dosing of bosutinib in pts with chronic phase chronic myeloid leukemia (CML) after second-generation tyrosine kinase

- inhibitor (TKI) therapy: results of the Bosutinib Dose Optimization (BODO) Study. *Annals of Hematology*, 102(10), 2741–2752. <https://doi.org/10.1007%2Fs00277-023-05394-0>
20. Henrich, M.T., Oertel, W.H., Surmeier, D.J. *et al.* Mitochondrial dysfunction in Parkinson's disease – a key disease hallmark with therapeutic potential. *Mol Neurodegeneration* 18(83), (2023). <https://doi.org/10.1186/s13024-023-00676-7>
21. Zhao, J., Wang, X., Huo, Z., Chen, Y., Liu, J., Zhao, Z., Meng, F., Su, Q., Bao, W., Zhang, L., Wen, S., Wang, X., Liu, H., & Zhou, S. (2022). The impact of mitochondrial dysfunction in amyotrophic lateral sclerosis. *Cells*, 11(13). <https://doi.org/10.3390%2Fcells11132049>
22. Brekk, O. R., Honey, J. R., Lee, S., Hallett, P. J., & Isacson, O. (2020). Cell type-specific lipid storage changes in Parkinson's disease patient brains are recapitulated by experimental glycolipid disturbance. *PNAS*, 117(44), 27646–27654. <https://doi.org/10.1073/pnas.2003021117>
23. Agrawal, I., Lim, Y.S., Ng, SY. *et al.* Deciphering lipid dysregulation in ALS: from mechanisms to translational medicine. *Translational Neurodegeneration*, 11(48), (2022). <https://doi.org/10.1186/s40035-022-00322-0>

## ACADEMIC VITA

**Lindsey Swanson**

lbs5560@psu.edu

### Education

Pursuing a Bachelor of Science in Biology: Genetics and Development Option

Pursuing a Minor in Economics

The Pennsylvania State University, Schreyer Honors College, University Park, PA

Anticipated Graduation: May 2024

### Work Experience

Penn State University Health Services, *Clinic Intern*, University Park, PA January 2023-present

- Collect patient intakes and vital signs
- Shadow physicians, physician assistants, and nurses during appointments and procedures

Lehigh Valley Health Network, *Intern*, Bethlehem, PA June-July 2022

- Worked with nurses and physicians in the Intensive Care Unit, Emergency Department, cardiac catheterization lab, and operating room
- Observed surgeries, trauma alerts, cardiac catheterizations, X-rays, MRIs, and other ICU procedures

Moravian Hall Square, *Personal Care Assistant, Medication Technician*, Nazareth, PA Oct. 2018-present

- Aid residents in daily tasks such as bathing, dressing, eating, and ambulating
- Administer oral, eye, nasal, and skin medications

Penn State University, *Learning Assistant*, University Park, PA Aug. 2022-May 2023

- Held 2 hours of LA sessions and office hours each week, attended weekly meetings with the professor and other members of the chemistry teaching team, attended all CHEM 112 lectures and assisted students during class

Penn State University, *Research Assistant*, University Park, PA Feb. 2023-present

- Research the mechanisms of Alzheimer's and Parkinson's diseases through experiments on *Drosophila*, cell culturing, and RNA sequencing

Nazareth Veterinary Center, *Veterinary Technician Assistant*, Nazareth, PA June-Aug. 2021

- Communicated with clients to take patient history and explain and distribute medications
- Obtained vital signs, restrained patients during appointments, observed surgical procedures, filled prescriptions, prepared vaccinations, prepared and read ear cytologies and other samples, ran blood tests

### Involvement

Penn State Dance Marathon, *Captain: Administrative Coordinator* Aug. 2022-May 2023

- Led portions of our weekly committee meetings and keep our 25 person committee informed on events and tasks that must be completed, plan committee events, design merchandise, coordinate THON blood drives
- Led a 26 member First Year Committee: held weekly meetings, taught first year students about THON, oversaw committee during THON-related events

Penn State Dance Marathon, *Captain: Alumni Communications Coordinator* Apr. 2023-present

- Oversee communication between Penn State and Penn State alumni regarding THON and write all emails that are sent to the 50,000+ alumni on THON's recipient list
- Lead a team of 5 other captains on an Alumni Communications team as well as coordinate events to keep alumni engaged in our current THON efforts

Orchesis Dance Company, *THON Finance Chair, Primary THON Chair* 2021-present

- Worked with businesses to plan fundraisers and order merchandise for Penn State THON, managed the THON money that we as a team of 35 dancers raised, and successfully led Orchesis in breaking our fundraising record of over \$30,000 as THON Finance Chair
  - Oversee 2 other THON Chairs as Primary THON Chair and spearhead Orchesis' THON efforts
- Alpha Epsilon Delta: Pre-Health Honors Society, *Service Subchair* 2021-present
- Planned weekly community service opportunities for the 400+ members in the club as subchair
  - Attained "Distinguished Member" status by reaching a certain level of attendance, community service, activity, and THON points and achieved national AED membership recognition

### **Awards**

- Dean's List 2020-present
- The President's Freshman Award 2021
- Awarded to Penn State students with a 4.0 GPA based on 12-36 credits earned
- Penn State Provost Scholarship 2020-present